Ecological Indicators 121 (2021) 107097

Contents lists available at ScienceDirect

Ecological Indicators

journal homepage: www.elsevier.com/locate/ecolind

Development of a toxicophenomic index for trace element ecotoxicity tests using the halophyte *Juncus acutus:* Juncus-TOX

Bernardo Duarte [a,b,*], Lorenzo Durante [a], João Carlos Marques [c], Patrick Reis-Santos [a,d], Vanessa F. Fonseca [a,e], Isabel Caçador [a,b]

[a] MARE – Marine and Environmental Sciences Centre, Faculty of Sciences of the University of Lisbon, Campo Grande, 1749-016 Lisbon, Portugal
[b] Departamento de Biologia Vegetal da Faculdade de Ciências da Universidade de Lisboa, Campo Grande, 1749-016 Lisboa, Portugal
[c] University of Coimbra, MARE – Marine and Environmental Sciences Centre, Department of Life Sciences, 3000 Coimbra, Portugal
[d] Southern Seas Ecology Laboratories, School of Biological Sciences, The University of Adelaide, SA 5005, Australia
[e] Departamento de Biologia Animal da Faculdade de Ciências da Universidade de Lisboa, Campo Grande, 1749-016 Lisboa, Portugal

ARTICLE INFO

Keywords:
Photobiology
JIP-test
Halophyte
Toxicophenomics
Ecotoxicity tests
Trace elements

ABSTRACT

Marine and coastal ecosystems are the ultimate sink of many contaminants from anthropogenic activities, such as trace elements. Although several ecotoxicological tests are available using autotrophic organisms, none focus on marine plants. *Juncus acutus* has already showed that it is a good candidate for ecotoxicological studies, providing a good set of contamination biomarkers. The present work evaluates the application of pulse amplitude modulated (PAM) fluorometry derived variables to develop an integrated biomarker response index (Juncus-TOX) and classify the exposure of *J. acutus* seedlings to trace element contamination. Trace element exposure (Zn, Cu, Cd, Ni, Pb, and As) led to reduced seedling growth, confirming the toxic effects imposed by the tested elements and concentrations. Observing the Kautsky curves derived from each metal exposure, an abrupt fluorescence decrease could be observed at high Cu, Pb and Ni concentrations, while As exposure caused a modification in the shape of the Kautsky curve, by increasing the intensity of the J-step. These changes have consequences in the whole variable dataset extracted from the Kautsky curves. With the exception of the seedlings exposed to Zn, the generated variables proved to be good classifiers of the level of exposure to which the plants were subjected. Moreover, the phenomological energy fluxes attained from this bio-optical approach highlight the photobiological impacts of the different trace elements, which together with metal-substituted chlorophyll generation, support the observed morphometric changes. Cadmium and As exposure increased significantly the absorbed and dissipated energy fluxs (ABS/CS and DI/CS). Regarding the trapped and electron transport energy flux (TR/CS and ET/CS) there was a substantial decreased in the seedlings exposed to the highest concentrations of Cu, Ni and Pb. The 42 bio-optical parameters extracted from the JIP-test were included in a toxicophenomic index (Juncus-TOX). All the computed index versions showed good correlations with the exogenous trace element dose. Thus, Juncus-TOX proved to be an efficient tool for application in ecotoxicological assays using *J. acutus*, highlighting the potential use of this species as a future halophyte model species for ecotoxicology.

1. Introduction

The relationship between increased human population density and environmental change in coastal regions is well known. Coastal water is the ultimate sink for an array of by-products of human activities. The EU's Task Group recommended that the achievement of Good Environmental Status under Descriptor 8 should be based upon monitoring programs covering the concentrations of chemical contaminants and also biological measurements relating to the effects of pollutants on marine organisms (Law et al., 2010), concluding that the combination of conventional and newer, effect-based methodologies, with the assessment of environmental concentrations of contaminants, provides a powerful and comprehensive approach.

At the basis of every marine system are phototrophs, cycling the

* Corresponding author at: MARE – Marine and Environmental Sciences Centre, Faculty of Sciences of the University of Lisbon, Campo Grande, 1749-016 Lisbon, Portugal.
E-mail address: baduarte@fc.ul.pt (B. Duarte).

https://doi.org/10.1016/j.ecolind.2020.107097
Received 17 August 2020; Received in revised form 13 October 2020; Accepted 16 October 2020
Available online 24 October 2020
1470-160X/© 2020 The Authors. Published by Elsevier Ltd. This is an open access article under the CC BY license (http://creativecommons.org/licenses/by/4.0/).

energy of the sun and soaking carbon, fuelling the trophic web, and therefore any disturbance at this level has inevitable impacts in the marine ecosystem. Contaminant toxic effects are known to have severe and specific effects in these organisms, especially impairing their photosynthetic metabolism (Anjum et al., 2016; Cabrita et al., 2017, 2016). This is a common feature to all marine phototrophs. Although these impacts are well described at the sub-cellular level for some contaminants, e.g. trace metals (Anjum et al., 2016; Cabrita et al., 2017; Santos et al., 2014), no photochemical-based ecotoxicity test and/or index has been developed. Remote sensing techniques like PAM fluorometry, LIF and spectroradiometry arise as potential non-invasive high-throughput screening (HTS) tools (Cabrita et al., 2017, 2016; Santos et al., 2015; 2014). These techniques use fluorescence and spectral signatures signals as a proxy of the phototroph. Any disturbance at the primary productivity level can be accurately assessed by these techniques (Duarte et al., 2017), which have proved to efficiently evaluate contaminants' effects at the physiological level with a dose-related response (Santos et al., 2014) and can additionally, be included into numerical indexes that can be easily used by stakeholders (Duarte et al., 2018; Duarte et al., 2017).

Trace elements are one of the most widespread sources of contamination present throughout the marine realm. These compounds are persistent in the environment and can have a serious detrimental impact by accumulating in the sediments (Caçador et al., 2009; Duarte et al., 2010), affecting their bioavailability (Duarte et al., 2013; Pedro et al., 2015a), and accumulating in plants and animals, which can ultimately lead to potential impacts in human health (Caçador et al., 2012; 2009;; Pedro et al., 2015b). Human activity and settlement in coastal areas have inevitably increased the sources of trace element contamination, allied with industrial, shipping and agricultural activities (Anjum et al., 2016; Duarte et al., 2010). Therefore, there is a reinforced necessity for highly efficient ecotoxicological trace element evaluation tools, especially directed to the marine realm and marine organisms. While several tests are available for freshwater plants and algae, no ecotoxicological tests have been developed for marine plants (OECD, 2011; Wang and Keturi, 1990).

Marine plants such as halophytes, are permanently subjected to high amounts of xenobiotics in their natural habitat, the salt marshes (Anjum et al., 2016; Duarte et al., 2010). These responses can be used as sentinel triggers that can be easily assessed via bio-optical techniques. *Juncus acutus,* in particular, has shown in the past to be easily cultivated under toxic exposure, presenting biochemical and biophysical traits with a high degree of correlation with the exposure dose, providing a good source of biomarkers (Mateos-Naranjo et al., 2019; 2014a, 2014b; Santos et al., 2015; Stefani et al., 1991). As abovementioned, bio-optical techniques, namely Pulse Amplitude Modulated (PAM) fluorometry, generate large datasets, in a fast and realiable way (Anjum et al., 2016; Duarte et al., 2017). While the high volume of data can represent an obstacle to the widespread application of these tools, it is also an advantage for bio-optical multivariate analysis, classification and index development (Duarte et al., 2017, 2019). Additionally, part of the data generated during the application of these tools can be directly applied for computing biologically relevant variables (Zhu et al., 2005), and can additionally be included in toxicophenomic indexes, easily communicated to stakeholders and managment authorities.

Having these features in mind, the present work aims to evaluate the application of PAM derived variables as multivariate classification tools using *J. acutus* as model halophyte species exposed to different trace elements and its concentrations. Moreover, the present work intents to test the inclusion of these PAM-derived variables in an integrated biomarker response index (Juncus-TOX) to classify *J. acutus* seedlings exposed to trace element contamination. As all the physiological features and mechanisms that underlie trace element exposure are already discussed elsewhere (Mateos-Naranjo et al., 2019, 2014; Santos et al., 2015; 2014;; Stefani et al., 1991), in the present paper the physiological implications and mode of action of the tested trace elements will be only addressed as potential traits to be included in a classification index and as potential descriptors of trace element exposure in halophytes.

2. Materials and methods

2.1. Seed harvest and incubations

Juncus acutus seeds were harvested in an undisturbed salt marsh of Tagus estuary within the old World Exposition 98′ site. All the collected flowers were brought to the laboratory and kept in dry conditions. Seeds were incubated in ¼ Hoagland solution supplemented with trace element salts (Sigma-Aldrich Ultra-Pure) of Zn ($ZnSO_4{\cdot}7H_2O$), Cu ($CuSO_4{\cdot}5H_2O$), Cd ($CdCl_2$), Ni ($NiCl_2$), Pb ($Pb(NO_3)_2$) and As ($Na_2HAsO_4{\cdot}7H_2O$) to attain the desired concentrations as described in Table 1. The selected elements are among the most commonly found in natural salt marsh environments (Caçador et al., 2009; Duarte et al., 2010). Trace element treatments were established targeting concentrations comparable to the ones detected in salt marsh environments (Caçador et al., 2009; Duarte et al., 2010). Approximately 20 seeds were placed in each petri dish with a Whatman GF/C filter as solid substrate. Each treatment (n = 3 petri dish, approx. 60 seeds) was soaked with 800 μL of the correspondent Hoagland solution supplemented with the corresponding trace element concentration solution. The addition of trace elements did not alter the pH of the Hoagland solution (pH = 5.6). The petri dishes were sealed with Parafilm and placed in a FytoScope Chamber (Photon System Instruments, Czech Republic) in the dark at 25 °C. Every three days, germinated seeds were counted until a maximum of 15 days. After germination (approximately after 6 days of incubation), the Petri dishes were placed in light conditions (150 μmol photons m^{-2} s^{-1}) in a 16 h/8h day-night regime using a sin function to simulate sunrise-midday-sunset conditions. At the end of the experiment, seedlings were collected and used for analysis. Seedlings were also weighed and measured for total length.

2.2. Pulse Amplitude Modulated (PAM) fluorometry

At the end of the experiment, Pulse Amplitude Modulated (PAM) midday chlorophyll fluorescence measurements were performed using a FluorPen FP100 (Photo System Instruments, Czech Republic), on 30 min dark-adapted individuals. Three replicates were always considered, as several previous works showed that this replication effort provides reliable data (Cabrita et al., 2017; Duarte et al., 2019; Santos et al., 2014; 2015). The polyphasic rise in fluorescence (OJIP) transient in dark-adapted individuals, was attained using the pre-programmed OJIP protocol of the FluorPen (Cabrita et al., 2017; Duarte et al., 2019). Table 2 summarizes the 42 parameters that were computed from the fluorometric data.

2.3. Juncus-TOX calculations

To understand global responses of *J. acutus* to different metals and exposure levels, a photochemical integrated biomarker response (IBR) was calculated according to Beliaeff and Burgeot (2002), posteriorly adapted by Broeg and Lehtonen (2006). Briefly, the Juncus-TOX index was calculated by summing up triangular star plot areas calculated for

Table 1
Different concentrations (mM) of the trace element treatments applied to the tested *J. acutus* seeds.

	Control	Low	Medium	High
Zn	0.002	5.0	7.0	10
Cu	0.0005	0.5	1.0	5.0
Cd	0.0	0.1	0.5	1.0
Ni	0.0	0.5	1.0	2.0
Pb	0.0	1.0	2.0	5.0
As	0.0	0.5	1.0	2.0

Table 2
Summary of fluorometric analysis parameters and their description.

Photosystem II Efficiency	
Fo	Basal fluorescence under weak actinic light in light and dark-adapted leaves
Fj	Fluorescence at 3 ms
Fi	Fluorescence at 30 ms
Fm	Maximum fluorescence measured after a saturating pulse in light and dark-adapted leaves
Fv	Variable fluorescence light (F'm – F'o) and dark (Fm – Fo) adapted leaves
Fk	Fluorescence at 300 ms
Vj	Variable fluorescence between the J-step and F0
Vi	Variable fluorescence between the I-step and F0
Vk	Variable fluorescence between the K-step and Fo
Wk	Amplitude of the K-step
Fm/Fo	Maximum fluorescence to basal fluorescence ratio
Fv/Fo	PSII potential activity
Fv/Fm	Quantum yield of primary photochemistry, equal to the efficiency by which a PS II trapped photon will reduce QA to Q-A
Electron Transport Chain (ETC) variables	
Mo	Net rate of PS II RC closure
Area	Corresponds to the oxidized quinone pool size available for reduction
Fix Area	Corresponds to the reduced quinone pool size available for oxidation
Sm	Quinone multiple turnover
Ss	Quinone sinlge turnover
N	Reaction centre turnover rate
Probabilistic variables	
ψPo	Maximum yield of primary photochemistry
Ψo	Probability of a PS II trapped electron to be transported from Q_A to Q_B
ψEo	Probability that an absorbed photon will move an electron into the electronic transport chain
ψDo	Quantum yield of the non-photochemical reactions
ψPav	Time to react the maximum fluorescence
Reaction Center-based Energy Fluxes	
Pi_Abs	Performance index
ABS/RC	Absorbed energy flux per reaction centre
TRo/RC	Trapped energy flux per reaction centre
ETo/RC	Electron transport energy flux per reaction centre
DIo/RC	Dissipated energy flux per reaction centre
Phenomological Energy Fluxes	
ABS/CS	Absorbed energy flux per excited cross section
TR/CS	Trapped energy flux per cross excited section
ET/CS	Electron transport energy flux per excited cross section
DI/CS	Dissipated energy flux per excited cross section
RC/CS	Oxidized reaction centres per excited cross section
Process variables	
PG	The grouping probability is a direct measure of the connectivity between the two PS II units
RE0/RC	Electron transport from PQH2 to the reduction of PSI end electron acceptors
RC/ABS	Reaction centre II density within the antenna chlorophyll bed of PSII
TR0/DI0	The contribution or partial performance due to the light reactions for primary photochemistry
(ψo/(1 – ψo)	Contribution of the dark reactions from Q_A^- to PC
δRo/(1 − δRo)	Contribution of PSI, reducing its end acceptors
ψEo/(1 − ψEo)	Equilibrium constant for the redox reactions between PSII and PSI
δRo	Electron movement efficiency from the reduced intersystem electron acceptors to the PS I end electron acceptors

each two neighbouring variables. To calculate IBR integrating all biomarkers, the general mean (m) and the standard deviation (s) of all data (including all metals and concentrations) regarding a given photochemical biomarker was calculated, followed by standardization to obtain Y:

$$Y = \frac{X - m}{s}$$

where X is the mean value for the biomarker at a given time. Then Z was calculated using Z = -Y or Z = Y, in the case of a biological effect corresponding respectively to an inhibition or a stimulation. Regarding the biological effect, biomarkers can either increase or decrease depending on the type and concentration of the metal exposure, but also vary among organisms. According to previous studies (Anjum et al., 2016; Duarte et al., 2017; Santos et al., 2015; 2014) the following was taken into consideration:

i) The fluorescence and amplitude of the K-step has its value increased in stress conditions, as a result of damages at the donor side of the PS II;
ii) The single and multiple quinone turnover rates (S_s and S_m) increase due to stress as a result of a slower quinone redox recycling activity;
iii) Reaction centre turnover rate (N) increases under stress as the reaction centre re-oxidation times are increased under stress;
iv) Quantum yield of the non-photochemical reactions (ψDo) increases under stress due to higher energy losses due to dissipation mechanisms;
v) The time to reach the maximum fluorescence (ψPav) is also increased under stress due to the slowdown of the PSII reaction centre re-oxidation rate;
vi) The dissipated energy fluxes (DI/RC and DI/CS) increase under stress as a result of a lower capacity of stressed chloroplasts to deal with the incoming light energy;
vii) The electron movement efficiency from the reduced intersystem electron acceptors to the PS I end electron acceptors (δRo) is also
viii) grouping probability (P_G), has its value increased as a result of a reduction of the connectivity between the two PS II units;
ix) all the remaining photochemical parameters are typically inhibited by metal exposure as a result of lower energy transduction capacity through the photosystems;

Subsequently, the score (S) was calculated as

$$S = Z + |Min|$$

where, S ≥ 0 and |Min| is the absolute value for the minimum value for all calculated Y for a given photochemical biomarker at all measurements made (again all metals and concentrations considered). Star plots were then used to display Score results (S) and to calculate the photochemical integrated biomarker response Juncus-TOX as:

$$Juncus - TOX = \sum_{t=15}^{n} A_i$$

being Ai the area between two consecutive clockwise scores in a given star plot:

$$A_i = \frac{S_i}{2}\sin\beta(S_i\cos\beta + S_{i+1}\sin\beta)$$

$$\beta = \tan^{-1}\frac{S_{i+1}\sin\alpha}{S_i - S_{i+1}\cos\alpha}$$

where S_i and S_{i+1} are two consecutive clockwise scores of a given star plot; n the number of photochemical biomarkers used and α:

$$\alpha = \frac{2\pi}{n}$$

Since the Juncus-TOX index value is obtained by summing up all the parameters, to allow correct and accurate future comparisons, the index was divided by the number of biomarkers used and presented as Juncus-$TOX_{Normalized}$ (Broeg and Lehtonen, 2006). Additionally, the variation of the index in an exposed sample (Juncus-$TOX_{Exposed}$) towards the control condition (Juncus-$TOX_{Control}$) was also calculated and expressed as:

$$\Delta Juncus - TOX = Juncus - TOX_{Control} - Juncus - TOX_{Exposed}$$

2.4. Statistical analysis

Due to the lack of data normality and homogeneity, the statistical analysis was based on non-parametric tests. To compare the effects of the tested metal exposures, a Kruskal-Wallis analysis of variance was performed using Statistica software (Statsoft). Significance was assumed when $p < 0.05$.

Multivariate statistical analysis was conducted using Primer 6 software (Clarke and Gorley, 2006), using non-parametric multivariate analysis packages. Data were normalized using the Primer 6 normalization algorithm and the normalization product was used to construct the respective resemblance matrixes based on the Euclidean distances between samples. The latter were used in a Canonical Analysis of Principal Coordinates (CAP) to generate statistical multivariate models based on the bio-optical inputs obtained from PAM analysis. This approach allows for the classification and separation of the different treatment groups. Additionally, CAP analysis performs a cross-validation step, providing a classification efficiency of the considered variables while descriptors of the applied stress. This multivariate approach is insensitive to heterogeneous data and frequently used to compare different sample groups using the intrinsic characteristics of

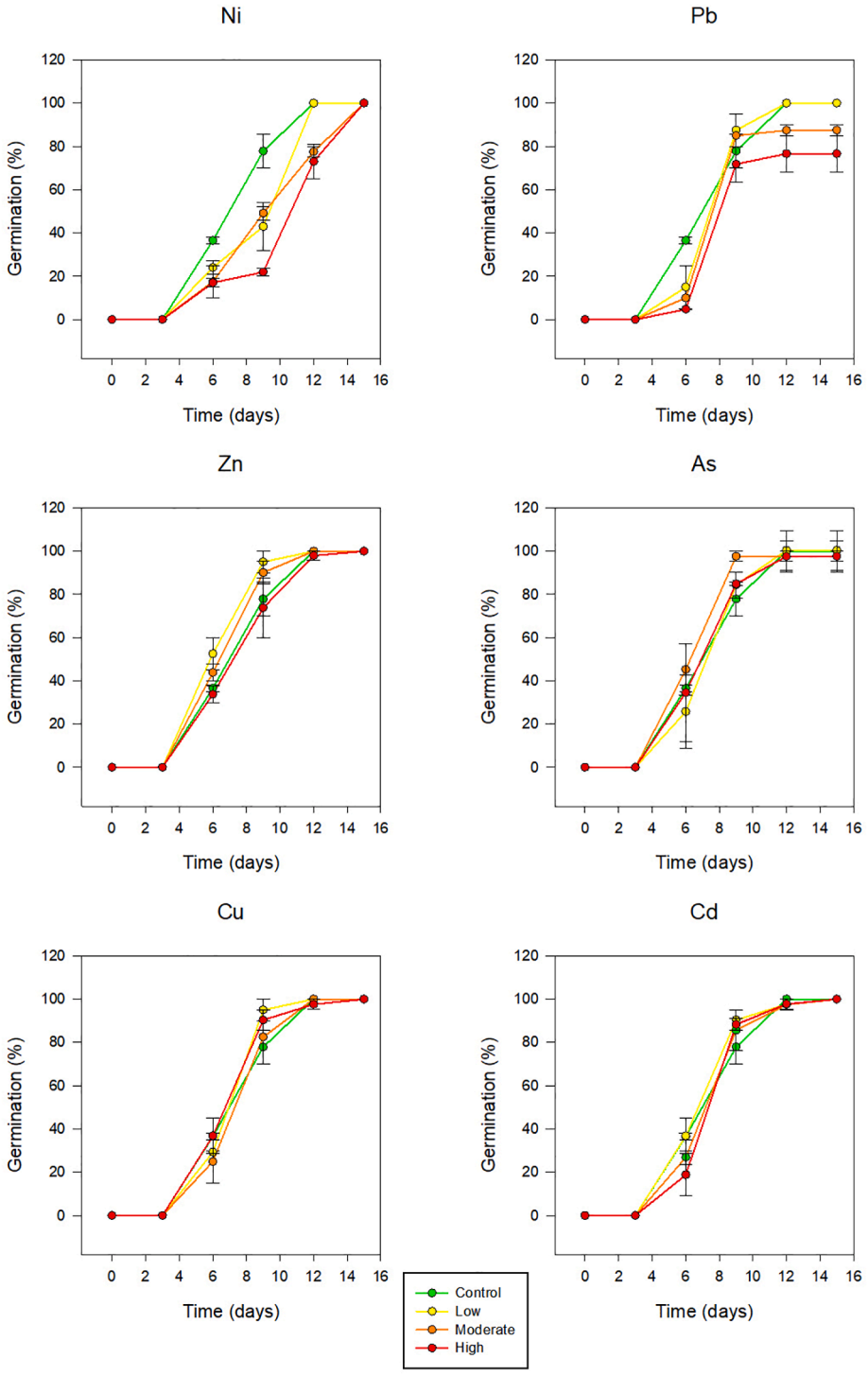

Fig. 1. Germination percentage along the incubation period for all the tested metals and concentrations (N = 5, average ± standard error).

each group (e.g. metabolic characteristics) (Cabrita et al., 2017; Duarte et al., 2017, 2019).

3. Results

3.1. Seed germination and morphometric characteristics

Overall, metal treatments lead to different outcomes concerning germination percentage (Fig. 1). In particular Zn, Cu and Cd acted similarly to nutrients at low and medium doses, slightly improving germination rate. However, the highest doses of these metals lead to a global decrease in the above-mentioned parameters. On the contrary, even at low concentrations, Ni and Pb were able to slow down the timing of seed germination when compared to control. Lead was the only trace element that caused a decrease in the germination percentage at the end of the exposure trial.

Using a morphometric analysis, it was possible to analyse the effects of the trace element exposure in seedling development (Fig. 2). Regarding the length of the germinated seedlings, Cu and Cd only produced significant effects at the highest dose, leading to a significant decrease in plant length (Fig. 2). On the other hand, Ni, As, and Pb lead to drastic reductions of the seedling length in all the tested concentrations. As for seedling biomass, it was significantly reduced under Cu, Ni, As and Pb exposure, whereas low concentrations of Cu and As seemed to promote biomass production.

3.2. Photobiological toxicity assessment

Observing the Kautsky curves derived from each metal exposure several differences are easily observable, especially concerning Cu, Pb, Ni, where an abrupt fluorescence decrease could be observed at high concentrations (Fig. 3). Moreover, As caused a modification in the shape of the Kautsky curve, by increasing the intensity of the J-step.

A canonical classification was performed using the bio-optical raw data obtained from the Kautsky curves measured in dark-adapted seedlings at the end of the exposure trials, considering all the tested metals and concentrations (Fig. 4). Except for Zn and Cu, all the tested trace elements showed a very clear grouping of the samples exposed to each of the tested concentrations. Considering the obtained classification efficiencies (Table 3), Cd, Ni, Pb and As presented 50%, 83.3%, 91.7% and 50% of correctly classified samples, respectively. Regarding the lower classification efficiencies obtained for Cd and As these are related to a misclassification of the control samples and of the samples exposed to the low concentration treatment. Regarding Cu-exposed samples, although the classification efficiency of the control samples and of the samples exposed to low and medium Cu concentrations, the samples exposed to the highest tested concentrations exhibited a 100% classification efficiency, contributing to the overall 58.3% classification efficiency of the Cu-exposed samples using the raw bio-optical data obtained.

Translating the induction curves into phenomological energy fluxes, it is possible to evaluate the effects of trace element exposure in the seedling photosynthetic metabolism, having as basis the four basic energy fluxes, as well as the number of PSII reaction centres available for light-harvesting (Fig. 5). Cadmium and As exposure lead to a significant increase in the absorbed energy flux (ABS/CS), while Cu, Ni and Pb had the inverse effect. Regarding the trapped energy flux (TR/CS) this was substantially decreased in the seedling exposed to the highest concentrations of Cu, Ni and Pb. Passing to the electron transport energy flux (ET/CS), all the maximum tested trace element concentrations induced a significant depletion of the energy flux. Moreover, in the seedlings exposed to Cu and Ni this effect was observable also in intermediate concentrations. Observing the seedlings dissipated energy flux (DI/CS), it was possible to detect a significant increase in Cd and As-exposed plants. On the other hand, Cu, Ni and Pb-exposed seedlings showed the inverse trend. Overlooking the number of oxidized reaction centres per seedling cross-section (RC/CS) it was possible to observe a significant decrease in this number in the seedling exposed to Cu, Ni and Pb highest concentrations. Arsenic-exposure lead to an increase in the seedlings RC/CS.

3.3. Metal-substituted chlorophylls

Observing the seedlings exposed to Zn, Cu and Cd it is possible to observe that these elements were included in the chlorophyll *a* and *b* molecules (Fig. 6). All the tested Zn and Cd concentrations produced a significant increase in the concentration of Zn and Cd-substituted chlorophyll *a* and *b*. The application of the two highest Cu concentrations also resulted in a significant increase in the concentration of Cu-substituted Chl *a*. As for Cu-substituted Chl *b*, all the tested Cu concentrations led to significant increases in this non-functional pigment concentration.

3.4. Juncus-TOX integrated biomarkers response index

An Integrated Biomarkers Response Index (IBR) was constructed using the whole bio-optical dataset (42 variables) generated by the application of JIP-test (Table S1). The generated index showed

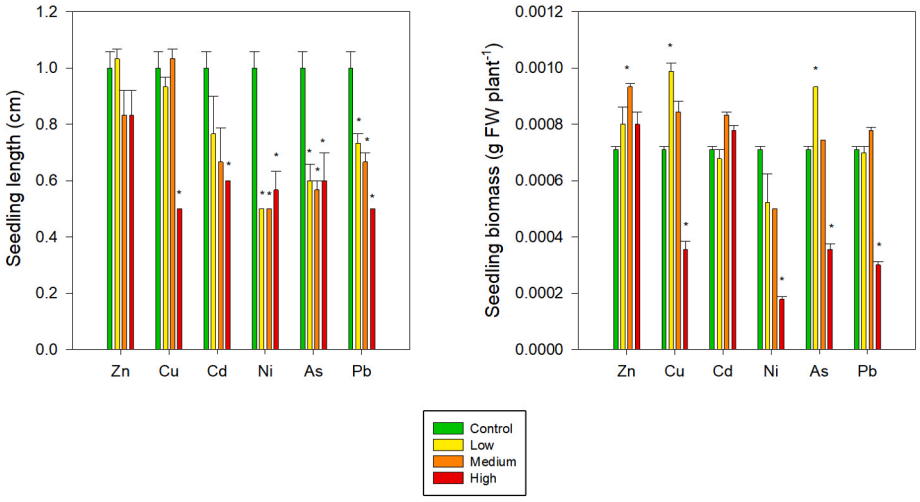

Fig. 2. Seedling length and weight at the end of the exposure trials for all the tested trace elements and concentrations (N = 5, average ± standard error, * denote significant differences towards the control at $p < 0.05$).

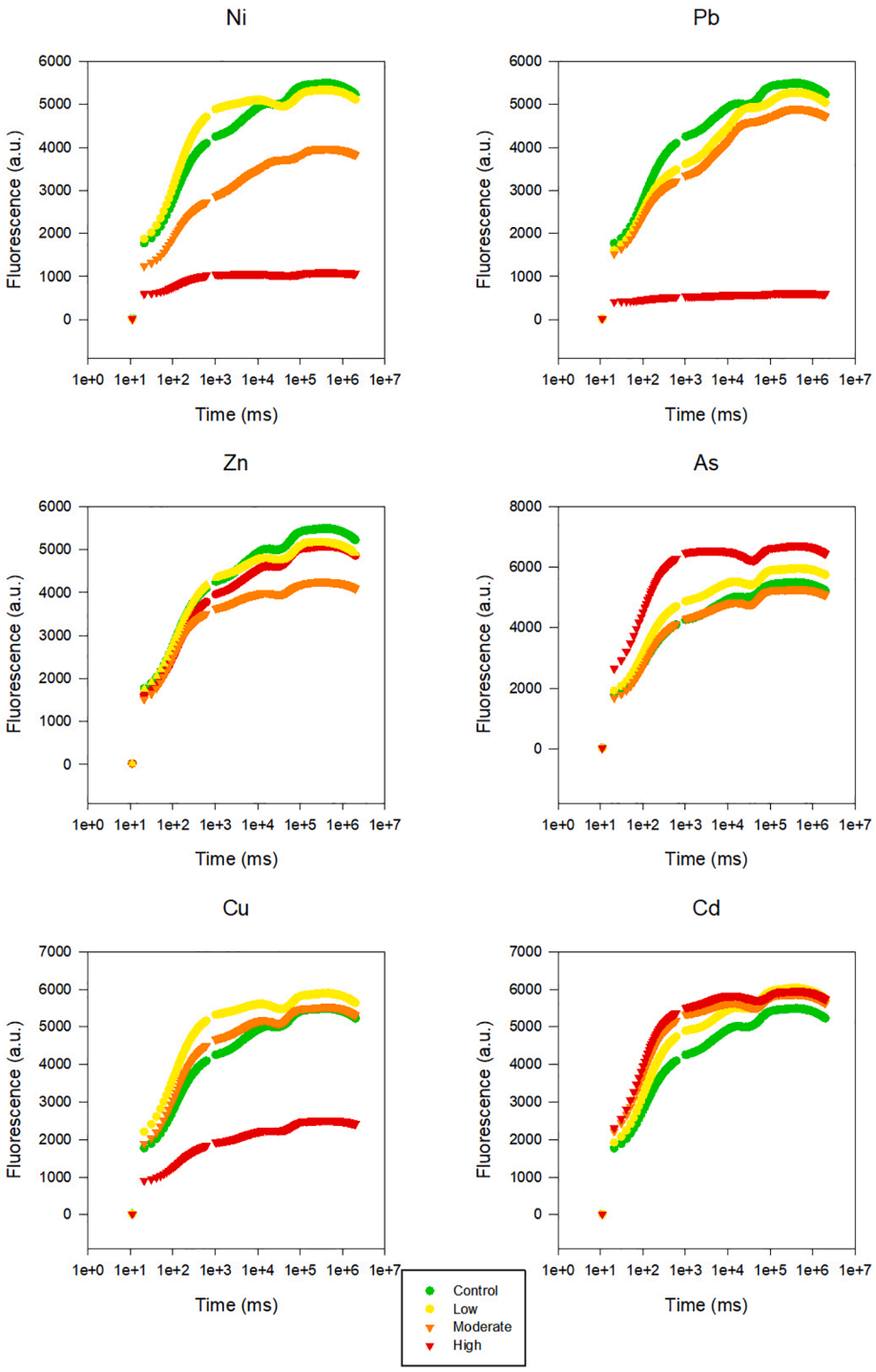

Fig. 3. Kautsky curves of dark-adapted seedlings at the end of the exposure trials for all the tested metals and concentrations (N = 5, average).

significant increases in all the seedlings exposed to the highest trace element doses but also in intermediate concentrations of Cd and Ni. The differences are maintained if the variation obtained between the index value of the test seedlings towards the control seedlings is observed (Fig. 7). Due to the very different orders of magnitude observed in the index computed for Ni and Pb, a normalized version of the index was also generated, dividing the index by the number of used variables. Again, the tendencies are maintained either using the index or its variation towards the control. With the exception of the seedlings exposed to Zn, all the versions of the index showed positive and significant correlations between the exogenous trace element concentration applied and the index value computed from the bio-optical variables (Table 4).

4. Discussion

Past studies have exposed *J. acutus* to trace elements (Cd and Zn), providing efficient biomarkers for acute trace element exposure, both in biophysical and biochemical terms (Mateos-Naranjo et al., 2019, 2014; Santos et al., 2015; 2014). This exposure in the natural environment also depends on the abiotic conditions of the sediments, namely oxygen and pH. As for the pH of the solutions this was kept unaffected and slightly acidic as the one found in salr marsh sediments colonized by halophytes

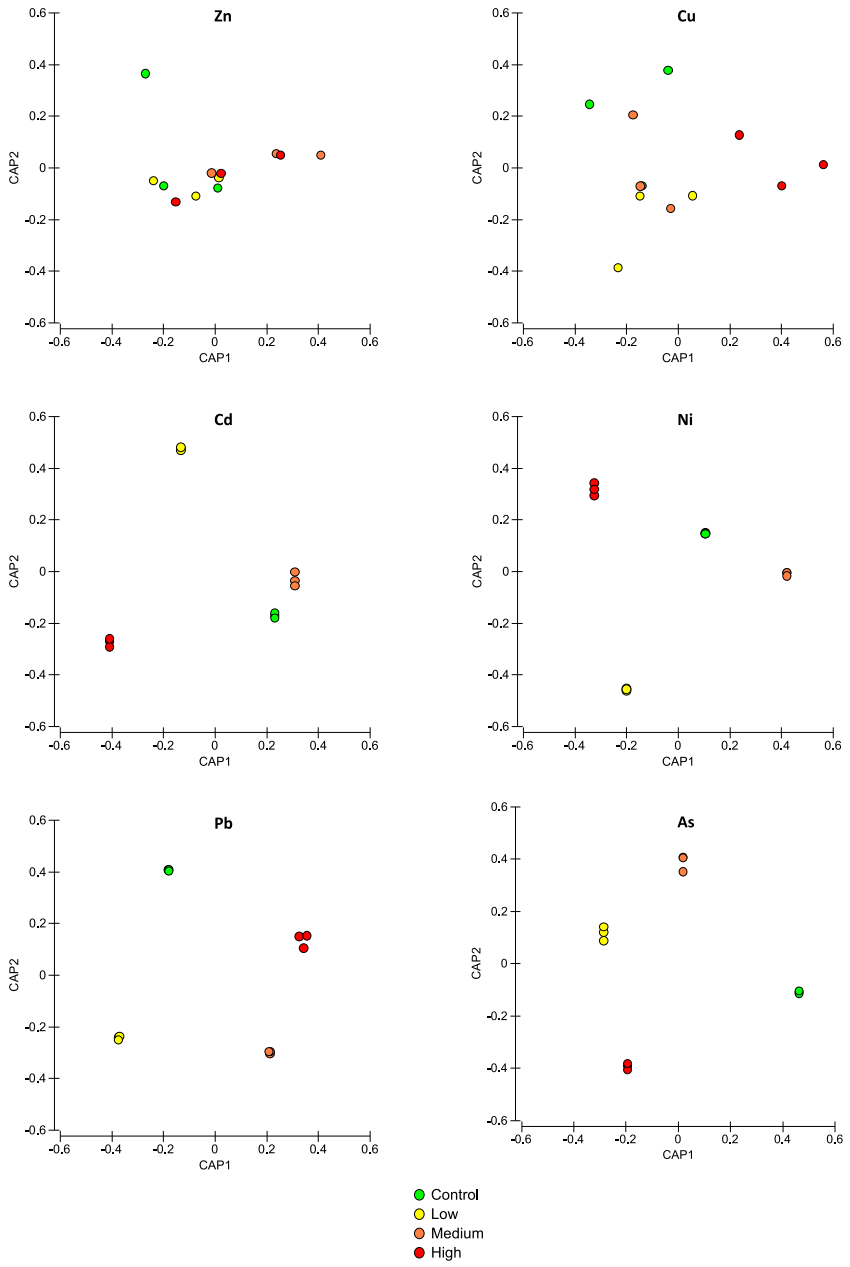

Fig. 4. Canonical Analysis of Principal Components (CAP) of the bio-optical raw data obtained from the Kautsky curves measured in dark-adapted seedlings at the end of the exposure trials for all the tested metals and concentrations.

(Caçador et al., 2009; Duarte et al., 2010). As for the oxygen, and although salt marsh sediments are often anoxic, in the halophyte rhizosphere there is an active pumping of atmospheric oxygen into the sediment by the plant, turing this an oxydized environment (Caçador et al., 2009; Duarte et al., 2010). This is specially critical for abnormal-valence heavy metals, sucha as As, and thus in the present study arsenate was employed as it is one of the most oxidized forms of As and thus more likely to occur in oxidized environmnets. Nevertheless, the bio-optical traits observed here under trace element exposure were never analysed as sources of data to be included in toxicophenomic tests and indexes. In the present work it is evident that trace element exposure leads to negative impacts on the seedlings physiology as denoted by the impacts observed both in the germination rates and in the morphological traits. As previously observed (Santos et al., 2015; 2014), trace element exposure leads to a significant effect on seedling elongation and biomass development, with observable reductions in the values of these traits with the tested trace element gradient dose. In isolation, these morphological traits are already indicative of toxicity and are common features used in similar toxicity assays (OECD, 2011), yet the very reduced seedling length and biomass can be prone to analytical errors and higher result variability due to methodological difficulties inherent to the analysis of small-sized seedlings. Nevertheless, these traits are toxicological evidence of the impacts of trace element exposure and thus can be used to validate the differences observed in terms of bio-optical data. The disturbances that occur at this level in response to trace metal pollution can be easily accessed through this technique, which uses chlorophyll *a* fluorescence signals as a proxy for the photosynthetic process (Strasser et al., 2000; Strasserf et al., 1995). In particular, the use of the JIP-test (name given from the three typical inflections observed in a Kautsky curve) has been extensively used in recent years. This is based

Table 3
Canonical classification efficiencies obtained from the bio-optical based CAP analysis measured in dark-adapted seedlings at the end of the exposure trials for all the tested metals and concentrations.

	Original group	Canonical Classification Group					Overall canonical classification efficiency
		Control	Low	Medium	High	%correct	
Zn	Control	1	1	0	1	33.3	25%
	Low	1	1	0	1	33.3	
	Medium	0	0	1	2	33.3	
	High	1	1	1	0	0	
Cu	Control	2	0	1	0	66.7	58.3%
	Low	0	1	2	0	33.3	
	Medium	1	1	1	0	33.3	
	High	0	0	0	3	100	
Cd	Control	0	1	2	0	0	50%
	Low	0	2	1	0	66.7	
	Medium	1	0	2	0	66.7	
	High	0	0	1	2	66.7	
Ni	Control	1	1	1	0	33.3	83.3%
	Low	0	3	0	0	100	
	Medium	0	0	3	0	100	
	High	0	0	0	3	100	
Pb	Control	2	0	0	1	66.7	91.7%
	Low	0	3	0	0	100	
	Medium	0	0	3	0	100	
	High	0	0	0	3	100	
As	Control	1	0	2	0	33.3	50%
	Low	0	1	1	1	33.3	
	Medium	0	1	2	0	66.7	
	High	0	1	0	2	66.7	

on the observed behaviour of fluorescence induction that occurs when a dark-adapted photosynthetic organ is illuminated, originating a profile with distinct phases (O, J, I, and P). These changes in fluorescence during the fast phase reflect the succession of events occurring in the electron transport chain (ETC), allowing for evaluation the photochemical process, including photon capture, energy transduction, and energy dissipation (Stirbet and Govindjee, 2011). This approach generates a high-volume of photochemical data with high relevance for physiological investigations but requires a high degree of expertise for its interpretation. Therefore, the inclusion of these variables in straightforward ecophysiological indexes has been successfully employed (Duarte et al., 2017) and revealed to be an efficient tool for ecosystem assessment (Stirbet et al., 2018).

The application of the JIP-test and the obtained Kautsky plots are composed by 460 fluorescence data points per sample, along a temporal axis. Observing these plots, it is evident that trace element exposure changes not only the curve shape but also its intensity at key fluorescence steps. These changes are due to the interaction of the tested trace elements with the different components of the photochemical apparatus (photosystems, electron transport chain and pigment molecules) (Anjum et al., 2016; Cabrita et al., 2017; Santos et al., 2015; 2014). Nevertheless, it is also evident that not all trace elements affect the photochemical profile in similar ways. This was already reported for marine diatoms, with some trace elements leading to severe impacts in the photochemical profiles, while other elements only produced slight changes in these biophysical traits (Cabrita et al., 2017, 2016). This is evident when these raw data (460 fluorescence points) are applied in a canonical classification. Elements such as zinc and copper did not produce significant effects in the Kautsky plots and thus did not generate any distinct sample groups according to the applied Zn or Cu exogenous dose. *Juncus acutus* is known to be a Zn-hyperaccumulator, and is resistant to high concentrations of this element via the activation of several anti-oxidant defence mechanisms (e.g. anti-oxidant enzymatic defences) (Mateos-Naranjo et al., 2014; Santos et al., 2014). Previous works with *J. acutus* exposed to higher Cu concentrations (15 and 23 mM Cu) also indicate that this plant is highly-tolerant to Cu exposure, even in its initial development phases (Mateos-Naranjo et al., 2019). Thus, considering this resistance/tolerance traits of this species to Zn and Cu is not surprising that at low concentration exposures, no evident photobiological differences were detected, leading to a low classification efficiency in the canonical analyses. Moreover, Cu and Zn are essential micronutrients with relevant metabolic functions in plants, and thus their toxicity ranges are higher than the tested concentrations (Hänsch and Mendel, 2009). Nickel is also known to be a micronutrient, nevertheless the tested environmentally relevant concentrations induced physiological changes in the tested seedlings. All the remaining tested trace elements do not have any known metabolic function in plant metabolism.

The 460 fluorescence data points that compose the Kautsky plot can be used to compute 42 variables with biological meaning (Strasser et al., 2000). From these, the phenomological energy fluxes are known to be efficient biomarkers of physiological stress conditions either imposed by natural abiotic origin (Duarte et al., 2017, 2015, 2014) or by contaminant exposure (Anjum et al., 2016; Cabrita et al., 2017; Duarte et al., 2019; Santos et al., 2014). Focusing on these five variables (absorbed, trapped, electron transport and dissipated energy fluxes and oxidized reaction centre density per illuminated cross-section), it is possible to evaluate the toxicological impacts of the tested trace elements and concentrations. The most widespread and evident changes due to trace element exposure was observed in the electron transport energy flux of the evaluated seedlings. All tested elements lead to a decrease in this energy flux. This is mostly due to the redox-dependency of the electron transport through the quinone-based electron transport chain (ETC), due to structural and functional changes in thylakoid membranes, reduced activity of ferrodoxin $NADP^+$ oxireductase and arrested plastoquinone synthesis (Barceló et al., 1988; Baszynki et al., 1980). A reduction in the number of oxidized reaction centres available to harvest light, and consequently reducing the absorbed and trapped energy flux was also observed. This was particularly evident in Cu, Ni and Pb exposed samples. Previous works showed that exposure to trace elements can lead to a decrease in the ratio of trimeric/monomeric light-harvesting complexes of the photosystem II (LHC II), reducing its ability to perform the quantum leaps necessary to harvest the incident photonic energy and convert it into an electron flow (Krupa, 1988). This led to the misleading effect of a reduction of the dissipated energy flux that could be perceived as a sign of unstressed conditions, but in fact, this reduction in the energy dissipation results from a simultaneous reduction of the absorbed energy flux, thus leaving a lower amount of energy to be dissipated. In samples exposed to Cu this fact can be also due to the substitution of the

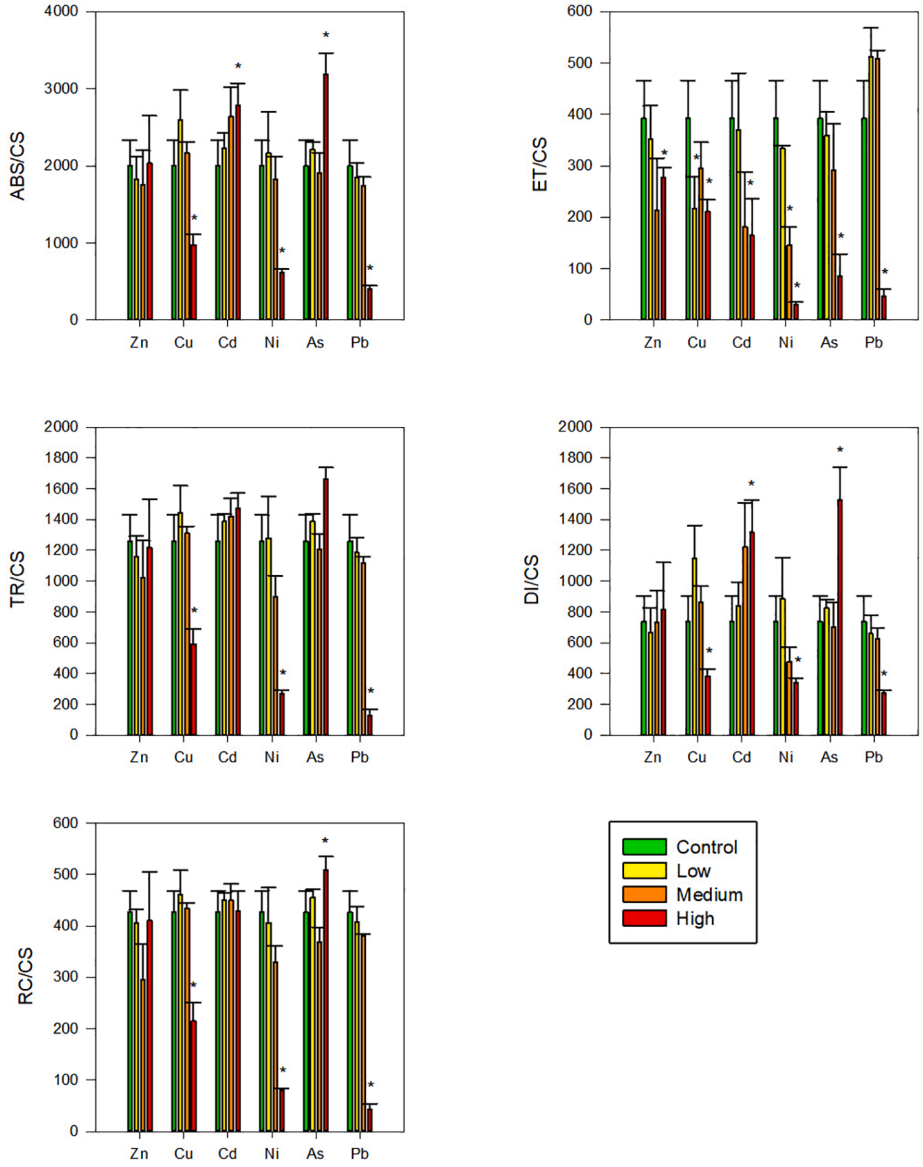

Fig. 5. Phenomological energy fluxes obtained from the seedlings at the end of the exposure trials for all the tested trace elements and concentrations (N = 5, average ± standard error, * denotes differences towards the control).

magnesium central atom in the chlorophyll *a* and *b* molecules by copper, reducing the ability of this non-functional substituted chlorophylls to harvest light (Peng et al., 2012). On the other hand, the substitution of the Mg atom in Chl *a* and *b* molecules by Zn and Cd, led to a different effect. In the seedlings where this substitution was observed there is a tendency for increasing energy dissipation, probably due to the lack of efficiency of these substituted molecules to convert the photonic energy into an electron flow, a mechanism that has been observed in *J. acutus* seedlings exposed to higher Cd and Zn doses (Santos et al., 2015; 2014). Overall the abovementioned phenomological traits indicate that the tested concentrations resulted in physiological changes concomitant with toxicity effects induced by trace element exposure.

Considering the photobiological changes induced by the trace element exposure trials, the derived 42 variables were evaluated within an integrated biomarker response index, here denominated Juncus-TOX. The resulting index intents to provide a single explanatory value than can be used and applied by, for instance, by stakeholders and competent authorities, responsible for ecosystem impact assessment programs or for ecotoxicology studies. Four different versions of the index were computed using normalized and non-normalized index variables (dividing the raw index by the 42 variables included) and its variation towards a control situation. The application of normalized index values provides a more homogenous range of results among the different trace elements (where the difference between the control and the most stressed sample is approximately 2.5), and is easier to compare and communicate to the non-scientific community (e.g. stakeholders, managers and authorities). In the same spirit, the use of the normalized variation towards the control (ΔJuncus-TOX$_{Normalized}$) reduces any potential misleading effect of index values several orders of magnitude above the control and eliminates the need to know the acceptable/realistic value of the index value in a control condition. Moreover, and because the gene pool of the seeds is not uniform over seasons and years, the ΔJuncus-TOX$_{Normalized}$ version also reduces any potential heterogeneous effect from different annual gene pools. Nevertheless, the assumption that all tests and control conditions should be performed with seeds from the same gene pool must be assured. Independently of the Juncus-TOX index version applied, and except for Zn and Cu, all the index values showed a significantly high correlation with the exogenous trace element concentration applied. As *J. acutus* is a Zn-hyperaccumulator (Santos et al., 2014) and thus the Zn exposure

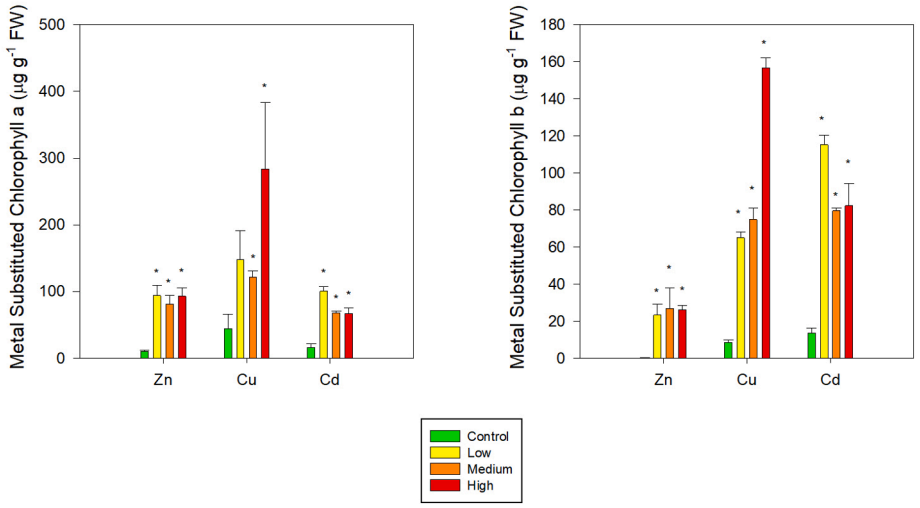

Fig. 6. Metal-substituted chlorophylls in the seedlings at the end of the exposure trials exposed to zinc, copper and cadmium at the different concentrations (N = 5, average ± standard error, * denotes differences towards the control).

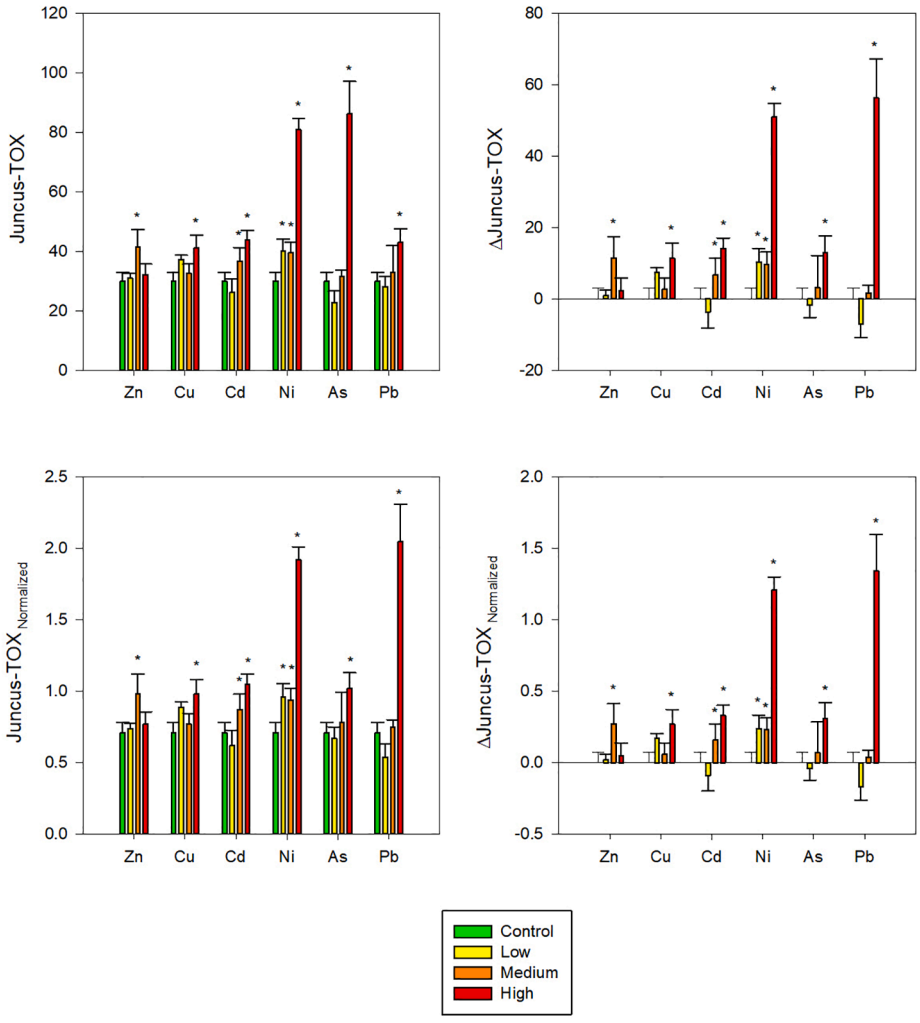

Fig. 7. Juncus-TOX index values (raw, normalized and its variation towards the control) calculated from the optical data obtained from the seedlings at the end of the exposure trials for all the tested trace elements and concentrations (N = 5, average ± standard error, * denotes differences towards the control).

concentrations tested (within relevant environmental ranges) are below the toxicity threshold, and thus there was no physiological feedback observable to the tested conditions.

5. Conclusion

The need to monitor coastal contamination supports the

Table 4
Spearman correlation coefficients (r^2) between the index values and the exogenous metal dose (* denotes significant correlation coefficients $p < 0.05$).

	Juncus-TOX	ΔJuncus-TOX	Juncus-$TOX_{Normalized}$	ΔJuncus-$TOX_{Normalized}$
Zn	0.41	0.41	0.41	0.41
Cu	0.82	0.82	0.82	0.82
Cd	0.96*	0.96*	0.96*	0.96*
Ni	0.94*	0.94*	0.94*	0.94*
As	0.93*	0.93*	0.93*	0.93*
Pb	0.93*	0.93*	0.93*	0.93*

development of novel tools to correctly and efficiently evaluate the impacts of contaminants in the marine biota. Bio-optical assessments have proved to be an efficient HTS tool to evaluate marine plants stress level, while providing significant insights on the metabolic processes underlying the physiological stress to which they are subjected. While for biologists and specifically for physiologists and ecotoxicologists, these physiological insights are essential to address the biochemical and biophysical relationships between halophytes and the environment, for stakeholders and monitoring programs supervisors a more practical approach is required. In this work, the developed Juncus-TOX toxicophenomic index, a quick and non-invasive analysis, which includes 42 bio-optical variables with biological meaning, proved to be an efficient tool to apply in ecotoxicological assays using *J. acutus* as model halophyte with a high degree of confidence for classifying the trace element exposure to which the test seedlings are exposed. This underpins the use of this species as a future halophyte model species for ecotoxicology.

CRediT authorship contribution statement

Bernardo Duarte: Conceptualization, Writing - original draft, Data curation, Project administration. **Lorenzo Durante:** Investigation. **João Carlos Marques:** Writing - review & editing. **Patrick Reis-Santos:** Writing - review & editing. **Vanessa F. Fonseca:** Formal analysis, Writing - review & editing. **Isabel Caçador:** Writing - review & editing.

Declaration of Competing Interest

The authors declare that they have no known competing financial interests or personal relationships that could have appeared to influence the work reported in this paper.

Acknowledgements

The authors would like to thank Fundação para a Ciência e a Tecnologia (FCT) for funding the research via project grants PTDC/CTA-AMB/30056/2017 (OPTOX) and UIDB/04292/2020. L. Durante work was financed by a Leonardo da Vinci Program grant. B. Duarte and V. Fonseca were supported by investigation contracts (CEECIND/00511/2017 and DL57/2016/CP1479/CT0024). P. Reis-Santos was supported by FCT through a postdoctoral grant (SFRH/BPD/95784/2013).

Appendix A. Supplementary data

Supplementary data to this article can be found online at https://doi.org/10.1016/j.ecolind.2020.107097.

References

Anjum, N.A., Duarte, B., Caçador, I., Sleimi, N., Duarte, A.C., Pereira, E., 2016. Biophysical and biochemical markers of metal/metalloid-impacts in salt marsh halophytes and their implications. Front. Environ. Sci. 4 https://doi.org/10.3389/fenvs.2016.00024.

Barceló, J., Vázquez, M.D., Poshenrieder, C., 1988. Structural and ultrastructural disorders in cadmium-treated bush bean plants (Phaseolus vulgaris L.). New Phytol. 108, 37–49. https://doi.org/10.1111/j.1469-8137.1988.tb00202.x.

Baszynki, T., Wajda, L., Król, M., Wolinska, D., Krupa, Z., Tukendorf, A., 1980. Photosynthetic activities of cadmium-treated tomato plants. Physiol. Plant. 48, 365–370. https://doi.org/10.1111/j.1399-3054.1980.tb03269.x.

Beliaeff, B., Burgeot, T., 2002. Integrated biomarker response: a useful tool for ecological risk assessment. Environ. Toxicol. Chem. 21, 1316–1322. https://doi.org/10.1002/etc.5620210629.

Broeg, K., Lehtonen, K.K., 2006. Indices for the assessment of environmental pollution of the Baltic Sea coasts: Integrated assessment of a multi-biomarker approach. Mar. Pollut. Bull. 53, 508–522. https://doi.org/10.1016/j.marpolbul.2006.02.004.

Cabrita, M.T., Duarte, B., Gameiro, C., Godinho, R.M., Caçador, I., 2017. Photochemical features and trace element substituted chlorophylls as early detection biomarkers of metal exposure in the model diatom Phaeodactylum tricornutum. Ecol. Indic. 0–1 https://doi.org/10.1016/j.ecolind.2017.07.057.

Cabrita, M.T., Gameiro, C., Utkin, A.B., Duarte, B., Caçador, I., Cartaxana, P., 2016. Photosynthetic pigment laser-induced fluorescence indicators for the detection of changes associated with trace element stress in the diatom model species Phaeodactylum tricornutum. Environ. Monit. Assess. 188 https://doi.org/10.1007/s10661-016-5293-4.

Caçador, I., Caetano, M., Duarte, B., Vale, C., 2009. Stock and losses of trace metals from salt marsh plants. Mar. Environ. Res. 67, 75–82. https://doi.org/10.1016/j.marenvres.2008.11.004.

Caçador, I., Costa, J.L., Duarte, B., Silva, G., Medeiros, J.P., Azeda, C., Castro, N., Freitas, J., Pedro, S., Almeida, P.R., Cabral, H., Costa, M.J., Caçador, I., 2012. Macroinvertebrates and fishes as biomonitors of heavy metal concentration in the Seixal Bay (Tagus estuary): Which species perform better? Ecol. Indic. 19, 184–190. https://doi.org/10.1016/j.ecolind.2011.09.007.

Clarke, K.R., Gorley, R.N., 2006. PRIMER v6: User Manual/Tutorial. Prim. Plymouth UK 192 p. https://doi.org/10.1111/j.1442-9993.1993.tb00438.x.

Duarte, B., Caetano, M., Almeida, P.R., Vale, C., Caçador, I., 2010. Accumulation and biological cycling of heavy metal in four salt marsh species, from Tagus estuary (Portugal). Environ. Pollut. 158, 1661–1668. https://doi.org/10.1016/j.envpol.2009.12.004.

Duarte, B., Carreiras, J., Pérez-Romero, J.A., Mateos-Naranjo, E., Redondo-Gómez, S., Matos, A.R., Marques, J.C., Caçador, I., 2018. Halophyte fatty acids as biomarkers of anthropogenic-driven contamination in Mediterranean marshes: Sentinel species survey and development of an integrated biomarker response (IBR) index. Ecol. Indic. 87, 86–96. https://doi.org/10.1016/j.ecolind.2017.12.050.

Duarte, B., Goessling, J.W., Marques, J.C., Caçador, I., 2015. Ecophysiological constraints of Aster tripolium under extreme thermal events impacts: Merging biophysical, biochemical and genetic insights. Plant Physiol. Biochem. 97, 217–228. https://doi.org/10.1016/j.plaphy.2015.10.015.

Duarte, B., Pedro, S., Marques, J.C., Adão, H., Caçador, I., 2017. Zostera noltii development probing using chlorophyll a transient analysis (JIP-test) under field conditions: Integrating physiological insights into a photochemical stress index. Ecol. Indic. 76, 219–229. https://doi.org/10.1016/j.ecolind.2017.01.023.

Duarte, B., Prata, D., Matos, A.R., Cabrita, M.T., Caçador, I., Marques, J.C., Cabral, H.N., Reis-Santos, P., Fonseca, V.F., 2019. Ecotoxicity of the lipid-lowering drug bezafibrate on the bioenergetics and lipid metabolism of the diatom Phaeodactylum tricornutum. Sci. Total Environ. 650, 2085–2094. https://doi.org/10.1016/j.scitotenv.2018.09.354.

Duarte, B., Santos, D., Caçador, I., 2013. Halophyte anti-oxidant feedback seasonality in two salt marshes with different degrees of metal contamination: Search for an efficient biomarker. Funct. Plant Biol. 40, 922–930. https://doi.org/10.1071/FP12315.

Duarte, B., Sleimi, N., Cagador, I., Caçador, I., Cagador, I., Caçador, I., 2014. Biophysical and biochemical constraints imposed by salt stress: Learning from halophytes. Front. Plant Sci. 5, 1–10. https://doi.org/10.3389/fpls.2014.00746.

Hänsch, R., Mendel, R.R., 2009. Physiological functions of mineral micronutrients (Cu, Zn, Mn, Fe, Ni, Mo, B, Cl). Curr. Opin. Plant Biol. 12, 259–266. https://doi.org/10.1016/j.pbi.2009.05.006.

Krupa, Z., 1988. Cadmium-induced changes in the composition and structure of the light-harvesting chlorophyll a/b protein complex II in radish cotyledons. Physiol. Plant. 73, 518–524. https://doi.org/10.1111/j.1399-3054.1988.tb05435.x.

Law, R., Hanke, G., Angelidis, M.O., Batty, J., Bignert, A., Dachs, J., Davies, I., Denga, Y., Duffek, A., Herut, B., Hylland, K., Lepom, P., Leonards, P., Mehtonen, J., Piha, H., Roose, P., Tronczynski, J., Velikova, V., Vethaak, D., 2010. Marine Strategy Framework Directive: Task Group 8 Report Contaminants and pollution effects. Joint Research Centre, European Commission. https://doi.org/10.2788/85887.

Mateos-Naranjo, E., Castellanos, E.M., Perez-Martin, A., 2014. Zinc tolerance and accumulation in the halophytic species Juncus acutus. Environ. Exp. Bot. 100, 114–121. https://doi.org/10.1016/j.envexpbot.2013.12.023.

Mateos-Naranjo, E., Pérez-Romero, J.A., Mesa-Marín, J., López-Jurado, J., Redondo-Gómez, S., 2019. Inter-population differences tolerance to Cu excess during the initials phases of Juncus acutus life cycle: implications for the design of metal restoration strategies. Int. J. Phytoremediation 21, 550–555. https://doi.org/10.1080/15226514.2018.1537242.

OECD, 2011. OECD Guidelines for the testing of Chemicals. Freshwater Alga and Cyanobacteria, Growth Inhibition Test. Organ. Econ. Coop. Dev. 1–25 https://doi.org/10.1787/9789264203785-en.

Pedro, S., Duarte, B., Raposo de Almeida, P., Caçador, I., 2015a. Metal speciation in salt marsh sediments: Influence of halophyte vegetation in salt marshes with different morphology. Estuar. Coast. Shelf Sci. 167, 248–255. https://doi.org/10.1016/j.ecss.2015.05.034.

Pedro, S., Duarte, B., Reis, G., Pereira, E., Duarte, A.C., Costa, J.L., Caçador, I., de Almeida, P.R., 2015b. Metal partitioning and availability in estuarine surface sediments: Changes promoted by feeding activity of Scrobicularia plana and Liza ramada. Estuar. Coast. Shelf Sci. 167, 240–247. https://doi.org/10.1016/j.ecss.2015.07.039.

Peng, H., Wang-Müller, Q., Witt, T., Malaisse, F., Küpper, H., 2012. Differences in copper accumulation and copper stress between eight populations of Haumaniastrum katangense. Environ. Exp. Bot. 79, 58–65. https://doi.org/10.1016/j.envexpbot.2011.12.015.

Santos, D., Duarte, B., Caçador, I., 2015. Biochemical and photochemical feedbacks of acute Cd toxicity in Juncus acutus seedlings: The role of non-functional Cd-chlorophylls. Estuar. Coast. Shelf Sci. 167, 228–239. https://doi.org/10.1016/j.ecss.2015.10.005.

Santos, D., Duarte, B., Caçador, I., 2014. Unveiling Zn hyperaccumulation in Juncus acutus: Implications on the electronic energy fluxes and on oxidative stress with emphasis on non-functional Zn-chlorophylls. J. Photochem. Photobiol. B Biol. 140, 228–239. https://doi.org/10.1016/j.jphotobiol.2014.07.019.

Stefani, A., Arduini, I., Onnis, A., 1991. Juncus acutus: germination and initial growth in presence of heavy metals. Ann. Bot. Fenn. 28, 37–43.

Stirbet, A., Govindjee,, 2011. On the relation between the Kautsky effect (chlorophyll a fluorescence induction) and Photosystem II: Basics and applications of the OJIP fluorescence transient. J. Photochem. Photobiol. B Biol. 104, 236–257. https://doi.org/10.1016/j.jphotobiol.2010.12.010.

Stirbet, A., Lazár, D., Kromdijk, J., Govindjee,, 2018. Chlorophyll a fluorescence induction: Can just a one-second measurement be used to quantify abiotic stress responses? Photosynthetica 56, 86–104. https://doi.org/10.1007/s11099-018-0770-3.

Strasser, R.J., Srivastava, A., Tsimilli-Michael, M., 2000. The fluorescence transient as a tool to characterize and screen photosynthetic samples, in: Probing Photosynthesis: Mechanism, Regulation & Adaptation. pp. 443–480.

Strasserf, R.J., Srivastava, A., Govindjee, 1995. Polyphasic chlorophyll a fluorescence transient in plants and cyanobacteria. Photochem. Photobiol. 61, 32–42. https://doi.org/10.1111/j.1751-1097.1995.tb09240.x.

Wang, W., Keturi, P.H., 1990. Comparative seed germination tests using ten plant species for toxicity assessment of a metal engraving effluent sample. Water. Air. Soil Pollut. 52, 369–376. https://doi.org/10.1007/BF00229444.

Zhu, X.G., Govindjee, Baker, N.R., DeSturler, E., Ort, D.R., Long, S.P., 2005. Chlorophyll a fluorescence induction kinetics in leaves predicted from a model describing each discrete step of excitation energy and electron transfer associated with Photosystem II. Planta 223, 114–133. https://doi.org/10.1007/s00425-005-0064-4.